^{1}H, ^{2}H, ^{19}F, ^{31}P, and ^{35}Cl NMR Studies on Molecular Motions in Ionic Plastic Phases of Pyrrolidinium Perchlorate and Hexafluorophosphate

Hiroshi Ono, Shin'ichi Ishimaru, Ryuichi Ikeda, and Hiroyuki Ishida[*,†]

Department of Chemistry, University of Tsukuba, Tsukuba 305 - 8571

†Department of Chemistry, Faculty of Science, Okayama University, Okayama 700 - 8530

(Received April 13, 1999)

Measurements of ^{1}H, ^{2}H, ^{19}F, ^{31}P, and ^{35}Cl NMR, differential scanning calorimetry (DSC), and X-ray powder diffraction were carried out in solid pyrrolidinium perchlorate ($[C_4H_8NH_2]ClO_4$) and hexafluorophosphate ($[C_4H_8NH_2]PF_6$). Five and three solid phases were obtained in perchlorate and hexafluorophosphate, respectively, by DSC measurement above 150 K. X-Ray powder patterns showed the highest-temperature solid phase of both salts to be CsCl-type cubic, indicating that both cations and anions take isotropically disordered orientations. The measurements of the NMR linewidth and its second moment revealed that the $C_4H_8NH_2^+$ and PF_6^- ions perform self-diffusion as well as isotropic rotation in this phase. From the dynamical behaviour of ions, the highest-temperature phase can be assigned to be an ionic plastic phase; this is the first example of an ionic plastic phase containing pyrrolidinium cations.

In previous studies, we have carried out ^{1}H, ^{2}H, ^{14}N, ^{31}P, and ^{35}Cl NMR, X-ray powder diffraction, and thermal measurements on piperidinium perchlorate, nitrate[1] and hexafluorophosphate[2] ($[C_5H_{10}NH_2]X$, X = ClO_4, NO_3, and PF_6), and revealed that the highest-temperature solid phases of these salts crystallize in cubic structures; the salts with the large anions (ClO_4^- and PF_6^-) form a CsCl-type cubic lattice, while that with small anion (NO_3^-) forms an NaCl-type. Isotropic rotations of both cations and anions were observed in these phases. Moreover, the onset of translational self-diffusion of the bulky cation and the PF_6^- anion in the CsCl-type cubic phase was detected by NMR. The ClO_4^- ion smaller in size is also expected to perform the same motion in this phase. We concluded that the CsCl-type cubic phase is the ionic plastic phase, because the dynamical behaviour of the constituent ions in this cubic phase is quite analogous to that in the plastic phase found in molecular crystals[3] and, at the same time, the entropy of fusion determined in these salts is low (7.9—11 $J\,K^{-1}\,mol^{-1}$) compared with 20 $J\,K^{-1}\,mol^{-1}$, which value has been accepted as the criterion for the formation of plastic phase.[3] Such ionic plastic phases have been recently shown to exist in various methyl- and ethyl-substituted ammonium salts.[4—25]

In the present investigation, we have undertaken studies on pyrrolidinium perchlorate ($[C_4H_8NH_2]ClO_4$) and hexafluorophosphate ($[C_4H_8NH_2]PF_6$) with the expectation of the ionic plastic phase being widespread in cyclic-alkylammonium salts. We measured differential scanning calorimetry (DSC), X-ray powder diffraction, ^{1}H and ^{19}F NMR spin-lattice relaxation times in the laboratory and rotating frame (T_1 and $T_{1\rho}$), spin-spin relaxation time (T_2), second moment (M_2) of ^{1}H and ^{19}F NMR linewidths, and ^{2}H, ^{14}N, ^{31}P, and ^{35}Cl NMR spectra.

Experimental

$[C_4H_8NH_2]ClO_4$ and $[C_4H_8NH_2]PF_6$ were prepared by neutralizing pyrrolidine with perchloric and hexafluorophosphoric acid, respectively. The obtained crystals of $[C_4H_8NH_2]ClO_4$ and $[C_4H_8NH_2]PF_6$ were recrystallized twice from ethanol and 1-propanol, respectively. Found: C, 28.17; H, 5.64; N, 8.15%. Calcd for $[C_4H_8NH_2]ClO_4$: C, 28.00; H, 5.87; N, 8.16%. Found: C, 21.93; H, 4.78; N, 6.39%. Calcd for $[C_4H_8NH_2]PF_6$: C, 22.13; H, 4.64; N, 6.45%. Before DSC and NMR measurements, both crystals were dried under vacuum (ca. 10^{-1} Pa) at 120 °C for 24 h. $[C_4H_8ND_2]ClO_4$ was prepared from purified $[C_4H_8NH_2]ClO_4$ by crystallization from D_2O three times and finally recrystallized from CH_3OD.

Differential scanning calorimetry (DSC) was carried out on a Seiko DSC 120 with a heating rate of 1 K min^{-1} from 150 K to the melting or the decomposition point. X-Ray powder patterns were taken at ca. 320 and 370 K for $[C_4H_8NH_2]ClO_4$ and ca. 300 K for $[C_4H_8NH_2]PF_6$ using a Philips X'Pert PW3050/00 diffractometer with Cu $K\alpha$ radiation.

The second moment of ^{1}H and ^{19}F NMR linewidths was recorded on a Bruker SXP 100 spectrometer with the solid-echo method.[26] T_1, $T_{1\rho}$ and T_2 of ^{1}H and ^{19}F NMR were measured on the SXP 100 and a home-made NMR spectrometer[27] with a JEOL ES-CC2 electromagnet. The inversion recovery method was used for the determination of T_1 and the Hahn's spin-echo method[28] for T_2. The radio-frequency field amplitude (H_1) of 0.4 mT was used for the $T_{1\rho}$ measurement. Experimental uncertainty was estimated to be within 10% for T_1, $T_{1\rho}$, and T_2. The temperature of the samples was controlled by a temperature control unit with an accuracy of 1 K.

^{2}H, ^{35}Cl, and ^{31}P NMR spectra were taken at Larmor frequencies of 46.07, 29.41, and 121.50 MHz, respectively, using a Bruker MSL 300 spectrometer. The $(\pi/2)_x - \tau - (\pi/2)_y - \tau$ method[29] was used for ^{2}H and ^{31}P NMR, while the Fourier transform after 90° pulse was

employed for ^{35}Cl NMR. ^{31}P NMR spectrum of 1.2% $[C_4H_8NH_2]$-PF_6 in a D_2O solution was obtained at room temperature using a JEOL JNM-EX270 spectrometer. 10% NaCl and 85% H_3PO_4 aqueous solutions were used as standards of ^{35}Cl and ^{31}P NMR spectra, respectively.

Results

Above 150 K, DSC measurements afforded five solid phases in $[C_4H_8NH_2]ClO_4$ and three phases in $[C_4H_8NH_2]$-PF_6. The obtained solid phases are designated as Phase I to V and Phase I to III for perchlorate and hexafluorophosphate, respectively, in the order of decreasing temperature. The phase transition temperatures from Phase V to IV in perchlorate and from Phase II to I in hexafluorophosphate were spread over ranges of 250—258 and 282—292 K, respectively, depending on the heating runs and samples. The observed transition temperatures (T_{tr}), the corresponding enthalpy changes (ΔH), and the entropy changes (ΔS) are summarized in Table 1.

X-Ray powder patterns were taken for perchlorate at ca. 370 K (Phase I) and ca. 320 K (Phase II), and for hexafluorophosphate at ca. 300 K (Phase I). Phases I and II of perchlorate were determined to be CsCl-type cubic (a = 5.837(2) Å, Z = 1, V = 198.9(2) Å^3, and D_x = 1.432(2) Mg m^{-3}) and tetragonal (a = 8.024(3), c = 6.098(2) Å, Z = 2, V = 392.6(4) Å^3, and D_x = 1.451(2) Mg m^{-3}), respectively. The structure in Phase I of hexafluorophosphate was determined to be CsCl-type cubic (a = 6.007(2) Å, Z = 1, V = 216.8(3) Å^3, and D_x = 1.662(3) Mg m^{-3}).

Figure 1 shows the temperature dependence of M_{2H} observed for perchlorate in the range 146—416 K. In Phase I, M_{2H} decreased to less than 0.01×10^{-2} mT^2 above 380 K. Figure 2 shows temperature dependences of M_{2H} and M_{2F} observed for hexafluorophosphate in the range 110—430 K. Above 413 K in Phase I, M_{2H} became less than 0.01×10^{-2} mT^2. M_{2F} in Phase I decreased with increasing temperature from 0.06×10^{-2} mT^2 (290 K) to less than 0.01×10^{-2} mT^2 above 390 K.

The ^{2}H spectrum of $[C_4H_8ND_2]ClO_4$ observed at 360 K (Phase I) showed a single peak with a half-height width of 300±10 Hz. ^{35}Cl NMR spectra of $[C_4H_8ND_2]ClO_4$ obtained at 315 K (Phase II) and 400 K (Phase I) also showed a single peak with a half-height width of 120±10 Hz. ^{31}P NMR spectra of $[C_4H_8NH_2]PF_6$ taken above 340 K (Phase I) gave septet peaks with a spin coupling constant $^1J_{PF}$ of 765 Hz. The chemical shift (δ) of the central peak was −147 ppm at 300 K from 85% H_3PO_4. The spectrum in D_2O solution of 1.2% $[C_4H_8NH_2]PF_6$ consists of the septet lines: $^1J_{PF}$ and δ were 707 Hz and −144 ppm, respectively.

Figure 3 shows temperature dependences of ^{1}H NMR T_1, $T_{1\rho}$, and T_2 (abbreviated to T_{1H}, $T_{1\rho H}$, and T_{2H}, respectively) of $[C_4H_8NH_2]ClO_4$. In Phase I, T_{1H} had a maximum at 380 K at a Larmor frequency of 48.9 MHz, while T_{1H} at 14.9 MHz decreased with increasing temperature. $T_{1\rho H}$ had a

Table 1. Transition Temperatures (T_{tr}), Enthalpy Changes (ΔH), and Entropy Changes (ΔS) in $[C_4H_8NH_2]X$ (X = ClO_4 and PF_6) Determined by DSC

Compound	T_{tr}/K	ΔH/kJ mol^{-1}	ΔS/J K^{-1} mol^{-1}
$[C_4H_8NH_2]ClO_4$	250—258	1.7±0.1	6.7±0.5
	306±1	3.7±0.2	12±1
	310±1	2.0±0.2	6.4±0.6
	342±1	0.97±0.04	2.8±0.2
	481[a]		
$[C_4H_8NH_2]PF_6$	244±1	3.7±0.5	15±2
	282—292	1.1±0.5	4.0±2.0
	555[b]	6.6±0.4	12±1

a) decomposed. b) mp with decomposition.

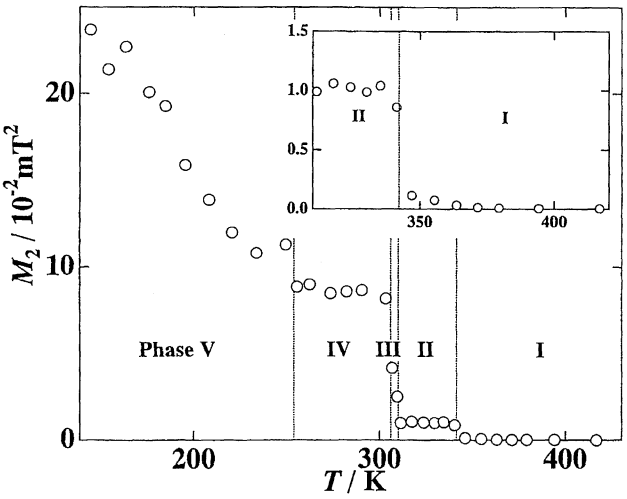

Fig. 1. Temperature dependence of the second moment (M_2) of ^{1}H NMR linewidth in $[C_4H_8NH_2]ClO_4$ at a Larmor frequency of 41 MHz. The broken lines show the phase transition temperatures determined by DSC. The temperature from Phase V to IV illustrated in this figure is 254 K.

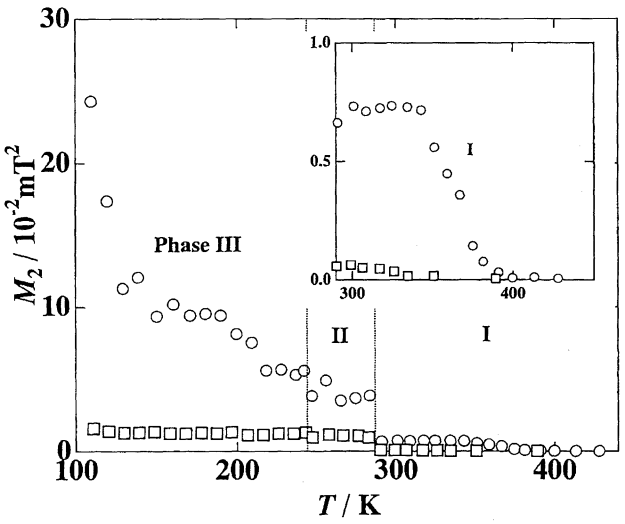

Fig. 2. Temperature dependences of the second moments (M_2) of ^{1}H and ^{19}F NMR linewidths observed in $[C_4H_8NH_2]PF_6$. M_{2H} observed at 36 MHz (○); M_{2F} at 34 MHz (□). The broken lines show the phase transition temperatures determined by DSC. The temperature from Phase II to I illustrated in this figure is 287 K.

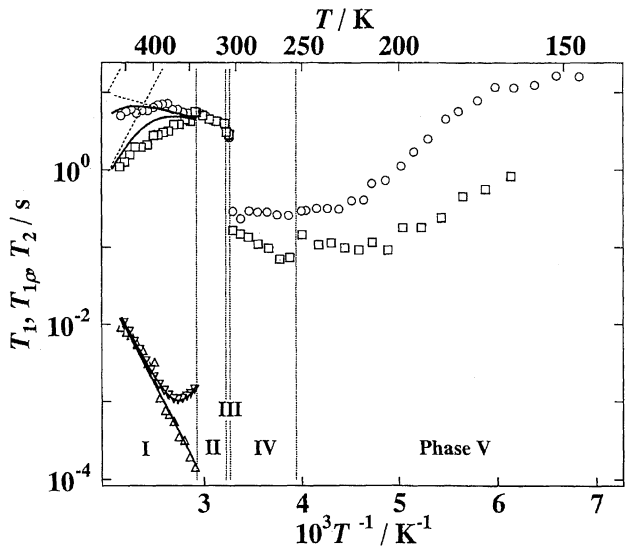

Fig. 3. Temperature dependences of ^{1}H NMR spin-lattice relaxation times in the laboratory and rotating frame (T_1 and $T_{1\rho}$), and spin–spin relaxation time (T_2) observed in $[C_4H_8NH_2]ClO_4$: T_{1H} at 48.9 MHz (○), T_{1H} at 14.9 MHz (□), $T_{1\rho H}$ at a locking field (H_1) of 0.4 mT (▽) and T_2 at 40.8 MHz (△). Solid and dotted lines are the best-fitted calculated values. The broken lines show the transition temperatures determined by DSC.

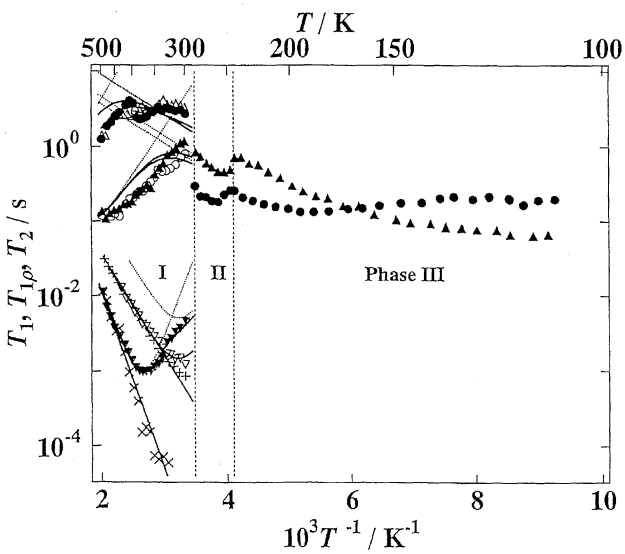

Fig. 4. Temperature dependences of the spin-lattice relaxation times in the laboratory (T_{1H} and T_{1F}), and rotating frame ($T_{1\rho H}$ and $T_{1\rho F}$), and spin–spin relaxation times (T_{2H} and T_{2F}) of ^{1}H and ^{19}F NMR observed in $[C_4H_8NH_2]PF_6$: T_{1H} at 40.7 MHz (○ and ●), T_{1F} at 38.3 MHz (▲ and △), T_{2H} at 40.7 MHz (×), T_{2F} at 38.3 MHz (+), $T_{1\rho H}$ (▼) and $T_{1\rho F}$ (▽) with a locking magnetic field (H_1) of 0.4 mT. Solid and dotted lines are the best-fitted calculated values. The broken lines show transition temperatures determined by DSC.

minimum value of 1.05 ms around 365 K and T_{2H} increased from 142 μs to 9.2 ms with temperature. $T_{1\rho H}$ and T_{2H} had almost the same values above 400 K. In Phases II and III, T_{1H} was independent of the Larmor frequency and increased upon heating.

Figures 4 and 5 show temperature dependences of T_{1H}, $T_{1\rho H}$, T_{2H}, and ^{19}F NMR T_1, $T_{1\rho}$, and T_2 (abbreviated to T_{1F}, $T_{1\rho F}$, and T_{2F}, respectively) in Phases I to III of $[C_4H_8NH_2]$-PF_6 and those in Phase I, respectively. In Phase I, T_{1H} and T_{1F} showed a marked non-exponential recovery of ^{1}H and ^{19}F magnetizations. This curve could be separated into two relaxation times, T_{1i}^s and T_{1i}^l ($T_{1i}^s < T_{1i}^l$, i = H or F), according to the equation:

$$(M_{0i} - M_{zi}(\tau))/2M_{0i} = A_s \exp(-\tau/T_{1i}^s) + A_l \exp(-\tau/T_{1i}^l), \quad (1)$$

where M_{0i} and $M_{zi}(\tau)$ are z components of the magnetization at thermal equilibrium and at the time τ after 180° pulse, respectively; A_s and A_l are constants ($A_s + A_l = 1$). $T_{1\rho H}$ showed a minimum value of 1 ms around 380 K. T_{2H} and T_{2F} increased upon heating and became 11 and 31 ms, respectively, at 500 K. $T_{1\rho H}$ and T_{2H} became nearly the same above 450 K, as did $T_{1\rho F}$ and T_{2F} above 340 K. In Phases II and III, T_{1H} and T_{1F} could be expressed by a single relaxation process.

Analysis and Discussion

The CsCl-type cubic structure in Phase I of $[C_4H_8NH_2]$-ClO_4 implies that both cations and anions are highly disordered, behaving like spherical ions in crystal. Isotropically rotating cations are also revealed from the narrow ^{2}H NMR spectrum. The quite narrow ^{35}Cl NMR spectra indicate that the rotation of anion occurs in Phase I as well as Phase II. In

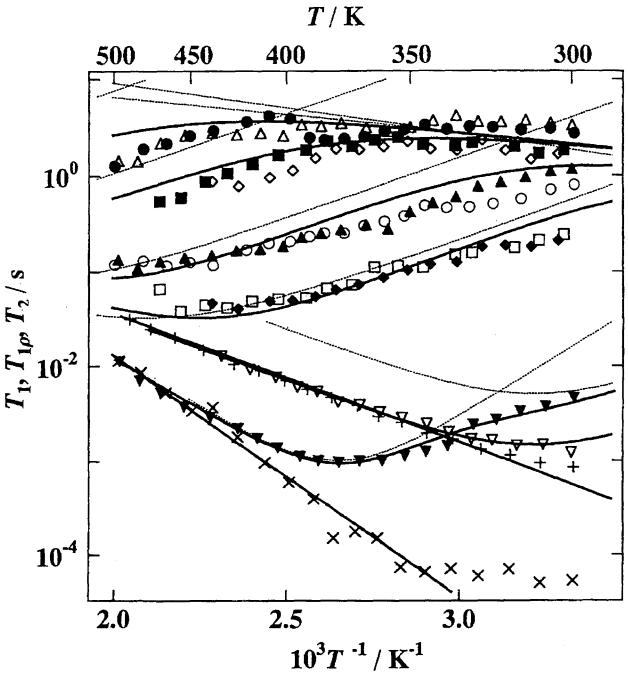

Fig. 5. Temperature dependences of the spin-lattice relaxation times in the laboratory (T_{1H} and T_{1F}) and rotating frame ($T_{1\rho H}$ and $T_{1\rho F}$), and spin–spin relaxation times (T_{2H} and T_{2F}) of ^{1}H and ^{19}F NMR in Phase I of $[C_4H_8NH_2]PF_6$: T_{1H} at 40.7 MHz (○ and ●) and at 15.0 MHz (□ and ■), T_{1F} at 38.3 MHz (▲ and △) and 14.1 MHz (◆ and ◇), $T_{1\rho H}$ (▼) and $T_{1\rho F}$ (▽) with the locking field (H_1) of 4.0 G, T_{2H} at 40.7 MHz (×), and T_{2F} at 38.3 MHz (+). Solid and dotted lines are the best-fitted calculated values.

addition to the isotropic rotation, the cation was found to perform the translational self-diffusion from the fact that M_{2H} in Phase I decreased to less than 0.01×10^{-2} mT^2 above 380 K (Fig. 1). This is because M_{2H} calculated for the isotropically rotating cations using the present X-ray data was 0.71×10^{-2} mT^2 and experimental values smaller than this can be only explained by the onset of the cationic self-diffusion. The anion smaller in size than the cation is also expected to perform the same motion.

The $T_{1\rho H}$ minimum and the increase in T_{2H} observed with increasing temperature in Phase I (Fig. 3) is attributed to the cationic self-diffusion, because the onset of this motion was shown above and the isotropic rotation of the cation is too fast to affect $T_{1\rho H}$ and T_{2H}. $T_{1\rho H}$ can be approximately expressed with the BPP-type equation[30] including the Torrey's treatment for the translational self-diffusion:

$$\begin{aligned}T_{1\rho H}^{-1} = C_{dif}\,[&(5/2)(\tau_{dif}/2)/\{1+\omega_{0H}^2(\tau_{dif}/2)^2\}\\ &+(\tau_{dif}/2)/\{1+4\omega_{0H}^2(\tau_{dif}/2)^2\}\\ &+(3/2)(\tau_{dif}/2)/\{1+4\omega_{1H}^2(\tau_{dif}/2)^2\}],\end{aligned} \quad (2)$$

$$\omega_{1H} = \gamma_H H_{1H}. \quad (3)$$

Here C_{dif}, ω_{0H}, and γ_H are the motional constant related to M_{2H} reduction due to the cationic self-diffusion, the Larmor frequency, and the gyromagnetic ratio of ^{1}H, respectively. τ_{dif} is the mean time interval between consecutive diffusional jumps of the cation, the temperature dependence of which is described by the Arrhenius-type equation expressed as

$$\tau_{dif} = \tau_{0,dif}\exp(E_a/RT), \quad (4)$$

where E_a and $\tau_{0,dif}$ are the activation energy and the correlation time at the infinite temperature, respectively. T_{2H} can be stated in terms of τ_{dif} under the condition of $\omega_{0H}\,\tau_{dif}\gg1$ as

$$T_{2H}^{-1} = (3/2)C_{dif}(\tau_{dif}/2). \quad (5)$$

Motional parameters, E_a, $\tau_{0,dif}$, and C_{dif}, determined by applying Eqs. 3, 4, and 5, are summarized in Table 2.

The frequency dependent T_{1H} observed in Phase I was explained by assuming the presence of the two relaxation processes given by

$$T_{1H}^{-1} = T_{1H,rot}^{-1} + T_{1H,dif}^{-1}, \quad (6)$$

where $T_{1H,rot}$ and $T_{1H,dif}$ are the relaxation times caused by the cationic isotropic rotation and the cationic self-diffusion, respectively. As mentioned above, τ_{rot} is short enough to satisfy the condition of $\omega_{0H}\,\tau_{rot}\ll1$, whereas τ_{dif} fulfils $\omega_{0H}\,\tau_{dif}\gg1$. Applying the BPP-equation[30] under these conditions, we can rewrite Eq. 6 as

$$T_{1H}^{-1} = 5C_{rot}\tau_{rot} + 2C_{dif}\omega_{0H}^{-2}(\tau_{dif}^{-1}/2), \quad (7)$$

where C_{rot} denotes the motional constant of isotropic rotation of cation. Assuming the temperature dependence of both τ_{rot} and τ_{dif} to be Arrhenius-type as expressed as Eq. 4, we evaluated activation energies for the cationic self-diffusion and isotropic rotation as shown in Table 2.

Table 2. Activation Energies (E_a), Correlation Times at the Limit of Infite Temperature (τ_0), and Motional Constants (C) Evaluated for Cationic Motions in Phase I of $[C_4H_8NH_2]ClO_4$

E_a/kJ mol^{-1}	τ_0/s	C/10^8 s^{-2}	Method	Motional mode
49±6			T_{2H}	
47±5	1.7×10^{-12}	4.2	$T_{1\rho H}$	Self-diffusion
47±5			T_{1H}	
7±2			T_{1H}	Isotropic rotation

The structure of $[C_4H_8NH_2]PF_6$ in Phase I is a CsCl-type cubic lattice isomorphous with that of perchlorate, implying that both cations and anions are dynamically disordered and obtain the greatest part of the motional freedom. In fact, the decrease in M_{2H} and M_{2F} to less than 0.01×10^{-2} mT^2 (Fig. 2) indicates that both ions perform self-diffusion as well as isotropic rotation in this phase, because these values are much smaller than the M_2 values ($M_{2H} = 0.93\times10^{-2}$ and $M_{2F} = 0.95\times10^{-2}$ mT^2) calculated for isotropically rotating cations and anions by using the present crystal data of Phase I. The liquid-like behaviour of the anions was also supported by the solid ^{31}P NMR spectra in Phase I showing septet peaks similar to the spectrum in the D_2O solution. The difference of $^1J_{PF}$, between 707 Hz in the solution and 765 Hz in the solid, is explainable in terms of the extension of P–F bond length caused by the polar solvent of D_2O. The high mobility of ions can also be derived from the entropy of fusion (12±1 J K^{-1} mol^{-1}) being lower than 20 J K^{-1} mol^{-1} as accepted as a criterion of forming the plastic phase in molecular crystals.[3]

According to the results of M_{2H} and M_{2F}, the T_{1H} and T_{1F} in Phase I of $[C_4H_8NH_2]PF_6$ (Fig. 5) can be explained in terms of the isotropic rotation and self-diffusion of both cations and anions. The minimum in $T_{1\rho H}$ and $T_{1\rho F}$, and the increase in T_{2H} and T_{2F} with temperature in Phase I are attributed to the cationic and anionic self-diffusion, respectively. Since the temperature dependency of the relaxation times in Phase I closely resembles that in the CsCl-type ionic plastic phase of $[C_5H_{10}NH_2]PF_6$, we analyzed the present data according to the procedure described in Ref. 2, where ^{1}H–^{1}H, ^{19}F–^{19}F, and ^{1}H–^{19}F magnetic dipolar interactions are taken into account.[31–34] Results of the analysis are summarized in Table 3.

The mean time intervals between consecutive diffusional jumps of the cation and anion, $\tau_{H,dif}$ and $\tau_{F,dif}$, extrapolated to the melting point were determined to be 1.2×10^{-7} and 1.1×10^{-7} s, respectively, using E_a and τ_0 obtained for the cationic and anionic self-diffusions listed in Table 5. The diffusion coefficients for the cation (D_H) and the anion (D_F) at the melting point were evaluated to be 5.0×10^{-13} and 5.5×10^{-13} m^2 s^{-2} from the relationship[3] given by

$$D_i = <r^2>/6\tau_{i,dif}, \quad (i = H \text{ or } F) \quad (8)$$

where $<r^2>$ denotes the mean-square-jump distance taken to be the squared unit cell distance in the CsCl-type cubic

Table 3. Activation Energies (E_a), Correlation Times at the Limit of Infite Temperature (τ_0), and Motional Constants (C) Evaluated for Cationic and Anionic Motions in Phase I of $[C_4H_8NH_2]PF_6$

E_a/kJ mol^{-1}	τ_0/s	$C/10^8$ s^{-2}	Method	Motional mode
45±3			T_{2H}	Cationic self-diffusion
42±1	1.3×10^{-11}	4.2 (C_{HH})	$T_{1\rho H}$	
42±1		4.2 (C_{HH})	T_{1H}	
		2.9 (C_{FF})		
		1.7 (C_{HF2})		
		1.2 (C_{FH1})		
26±2			T_{2F}	Anionic self-diffusion
26±2	4.0×10^{-10}	2.9 (C_{FF})	$T_{1\rho F}$	
		0.42 (C'_{HF})	$T_{1\rho H}$	
24±2		4.2 (C_{HH})	T_{1F}	
		2.9 (C_{FF})		
		1.7 (C_{HF2})		
		1.2 (C_{FH1})		
7±3			T_{1H}	Cationic isotropic rotation
10±3			T_{1F}	Anionic isotropic rotation

lattice. The obtained τ and D values are close to those reported in the molecular plastic crystals.[3,35] Furthermore, we should note that $\tau_{H,dif}$ and $\tau_{F,dif}$, or D_H and D_F, become almost the same value at the melting point, in spite of the large differences in the diffusion rate between cations and anions in the low temperature range of Phase I and in the size of the ions. The same result has been obtained for the melting in $[C_5H_{10}NH_2]PF_6$ which forms the ionic plastic phase of CsCl-type.[2] This fact suggests that the melting of ionic crystal occurs when the diffusional rates of both cation and anion reach a certain threshold value.

Figure 6 illustrates the relationship between the activation energy for self-diffusion and the lattice constant determined for CsCl-type cubic phase of alkylammonium perchlorate and hexafluorophosphate. We can see a tendency that the activation energy of the cation increases with increasing the lattice size, implying that the increase in molecular weight and size makes the diffusion difficult. Furthermore, the activation energy of PF_6^- ions shows an analogous size dependency to that in the cation. Since the activation energy for self-diffusion is related to the potential barrier for the ion to jump into a neighbouring vacant site and also to the energy for vacancy formation,[3,35] this result suggests that cation and anion vacancies are not formed independently but with some correlation, probably as a cation and anion vacancy pair and/or a Schottky defect.

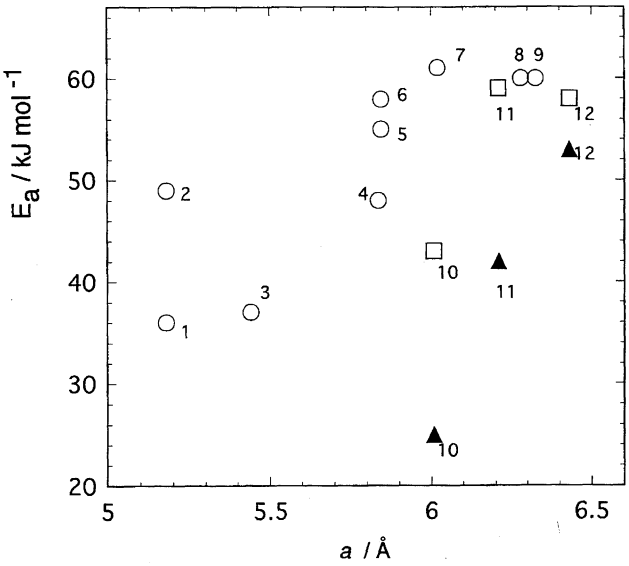

Fig. 6. Activation energies for ionic self-diffusion versus lattice constants in CsCl-type ionic phase of alkylammonium perchlorate and hexafluorophosphate. ○: cation in perchlorate; □: cation in hexafluorophosphate; ▲: anion in hexafluorophosphate. 1: $CH_3NH_3ClO_4$;[12,36] 2: $CH_3NH_3ClO_4$;[7] 3: $(CH_3)_2NH_2ClO_4$;[8,36] 4: $C_4H_8NH_2ClO_4$; 5: $(CH_3)_3NHClO_4$;[23] 6: $(CH_3)_3NHClO_4$;[6,37] 7: $C_5H_{10}NH_2ClO_4$;[1] 8: $(CH_3)_3NC_2H_5ClO_4$;[24] 9: $(CH_3)_3NC_2H_4OHClO_4$;[25] 10: $C_4H_8NH_2PF_6$; 11: $C_5H_{10}NH_2PF_6$;[2] 12: $(CH_3)_3NC_2H_5PF_6$.[24]

Conclusion

In the present investigation, we have revealed that the highest-temperature solid phases of $[C_4H_8NH_2]ClO_4$ and $[C_4H_8NH_2]PF_6$ crystallize in CsCl-type cubic lattices. Isotropic rotations of both cations and anions were observed in these phases. Moreover, self-diffusion of the bulky $C_4H_8NH_2^+$ ion and the PF_6^- ion was definitely detected by NMR. It is highly possible that the smaller anion, ClO_4^-, also diffuses in the cubic phase. Since the dynamical properties of the constituent ions in cubic phases are quite analogous to those in the plastic phase found in molecular crystals, these solid phases can be assigned to the ionic plastic phase. To our knowledge, this is the first report on the ionic plastic phase consisting of $C_4H_8NH_2^+$ cations.

The authors are grateful to Dr. T. Nakahodo and Prof. N. Furukawa for the use of a JEOL JNM-EX270 in University

of Tsukuba. This work was supported by Grants-in-Aid for Scientific Research (B) Nos. 09440234, 1014907, and 10440208 from the Ministry of Education, Science, Sports and Culture.

References

1 H. Ono, S. Ishimaru, R. Ikeda, and H. Ishida, *Chem. Phys. Lett.*, **275**, 485 (1997).

2 H. Ono, S. Ishimaru, R. Ikeda, and H. Ishida, *Ber. Bunsen-Ges. Phys. Chem.*, **102**, 650 (1998).

3 "The Plastically Crystalline State," ed by J. N. Sherwood, Wiley, New York (1979).

4 H. Ishida, R. Ikeda, and D. Nakamura, *Chem. Lett.*, **1982**, 1943.

5 H. Ishida, R. Ikeda, and D. Nakamura, *Phys. Status Solidi (A)*, **70**, K151 (1982).

6 S. Jurga, *Phys. Status Solidi (A)*, **81**, 77 (1984).

7 S. Jurga and H. W. Spiess, *Z. Naturforsch., A*, **40a**, 602 (1985).

8 S. Jurga and H. W. Spiess, *Ber. Bunsen-Ges. Phys. Chem.*, **89**, 763 (1985).

9 H. Ishida, R. Ikeda, and D. Nakamura, *J. Chem. Soc., Faraday Trans. 2*, **81**, 963 (1985).

10 H. Ishida, R. Ikeda, and D. Nakamura, *Bull. Chem. Soc. Jpn.*, **59**, 915 (1986).

11 S. Jurga, G. S. Harbison, B. Blümich, H. W. Spiess, F. Fujara, and A. Olinger, *Ber. Bunsen-Ges. Phys. Chem.*, **90**, 1153 (1986).

12 H. Ishida, R. Ikeda, and D. Nakamura, *Bull. Chem. Soc. Jpn.*, **60**, 467 (1987).

13 M. Tansho, D. Nakamura, and R. Ikeda, Z. *Naturforsch., A*, **44a**, 738 (1989).

14 T. Tanabe, R. Ikeda, and D. Nakamura, *Phys. Status Solidi (A)*, **114**, K143 (1989).

15 T. Tanabe, R. Ikeda, and D. Nakamura, *J. Chem. Soc., Faraday Trans.*, **87**, 987 (1991).

16 M. Tansho, D. Nakamura, and R. Ikeda, *J. Chem. Soc., Faraday Trans.*, **87**, 3255 (1991).

17 M. Tansho, D. Nakamura, and R. Ikeda, *Ber. Bunsen-Ges. Phys. Chem.*, **95**, 1643 (1991).

18 H. Ishida, N. Hayama, and R. Ikeda, *Chem. Lett.*, **1992**, 1333.

19 H. Ishida, T. Iwachido, and R. Ikeda, *Ber. Bunsen-Ges. Phys. Chem.*, **96**, 1468 (1992).

20 H. Ono, R. Seki, R. Ikeda, and H. Ishida, *J. Mol. Struct.*, **345**, 235 (1995).

21 H. Ishida, Y. Furukawa, S. Kashino, S. Sato, and R. Ikeda, *Ber. Bunsen-Ges. Phys. Chem.*, **100**, 433 (1996).

22 H. Ono, R. Ikeda, and H. Ishida, *Ber. Bunsen-Ges. Phys. Chem.*, **100**, 1833 (1996).

23 H. Ishida and Y. Furukawa, *Z. Naturforsch., A*, **51a**, 83 (1996).

24 H. Ono, S. Ishimaru, R. Ikeda, and H. Ishida, *Bull. Chem. Soc. Jpn.*, **70**, 2963 (1997).

25 H. Ishida, M. Kato, H. Ono, and R. Ikeda, *Z. Naturforsch., A*, **52a**, 637 (1997).

26 J. G. Powles and J. H. Strange, *Proc. Phys. Soc.*, **82**, 6 (1963).

27 T. Kobayashi, H. Ohki, and R. Ikeda, *Mol. Cryst. Liq. Cryst.*, **257**, 279 (1994).

28 E. L. Hahn, *Phys. Rev.*, **80**, 580 (1950).

29 J. H. Davis, K. R. Jeffery, M. Bloom, and M. I. Valic, *Chem. Phys. Lett.*, **42**, 390 (1976).

30 A. Abragam, "The Principles of Nuclear Magnetism," Oxford University Press, London (1961).

31 S. Albert and H. S. Gutowsky, *J. Chem. Phys.*, **59**, 3585 (1973).

32 D. E. O'Reilly, E. M. Peterson, and T. Tsang, *Phys. Rev.*, **160**, 333 (1967).

33 Y. Furukawa and H. Kiriyama, *Bull. Chem. Soc. Jpn.*, **52**, 339 (1979).

34 S. Sato, M. Kondo, R. Ikeda, and D. Nakamura, *Ber. Bunsen-Ges. Phys. Chem.*, **93**, 450 (1989).

35 J. M. Chezeau and J. H. Strange, *Phys. Rep.*, **53**, 1 (1979).

36 M. Stammler, R. Bruenner, W. Schmidt, and D. Orcutt, *Adv. X-ray Anal.*, **9**, 170 (1966).

37 H. Ishida, Y. Kubozono, S. Kashino, and R. Ikeda, *Z. Naturforsch., A*, **49a**, 723 (1994).